Proceedings of the 6th Nordic Signal Processing Symposium - NORSIG 2004
June 9 - 11, 2004
Espoo, Finland

Comparison of Pattern Classification Methods in Segmentation of Dynamic PET Brain Images

Heidi Koivistoinen, Jussi Tohka, and Ulla Ruotsalainen

Institute of Signal Processing, Tampere University of Technology, P.O. Box 553, 33101 Tampere, FINLAND
Email: heidi.koivistoinen@tut.fi, jussi.tohka@tut.fi, ulla.ruotsalainen@tut.fi

ABSTRACT

In this study, pattern classification methods for automatic segmentation of PET brain receptor density images are compared. Because of low contrast to noise ratio we utilize information about dynamics of tracer uptake present in PET studies. We compare three methods: expectation-maximization algorithm (EM), fuzzy C-means algorithm (FCM) and independent component analysis (ICA). Particularly, our interest was in segmentation of the striatum and cerebellum structures. The methods were applied to a Monte Carlo simulated phantom image and to five different human PET studies. We were able to extract striatum with the EM algorithm and ICA satisfactorily from all PET studies. With the FCM algorithm striatum could not be differentiated to its own class. The cerebellum was found only with ICA from the simulated image. ICA seemed to be less sensitive to noise of all the studied methods. The EM algorithm was most sensitive to patient movement in the human PET studies. The EM algorithm and ICA seemed promising for the segmentation task when taking low contrast to noise ratios of the PET images into account.

I. INTRODUCTION

The aim of this work is comparison of automatic methods for segmentation of positron emission tomography (PET) data by exploiting all information of a PET study. The three-dimensional (3-D) PET brain images considered in this study represent receptor density of the brain. A dynamic PET study contains information about dynamics of tracer uptake related to brain structures, i.e. a dynamic PET study is a sequence of 3-D images acquired during subsequent time intervals. For a human viewer, segmentation of dynamic images is impossible because it demands ability to examine 4-D data (three dimensions and time) with noise and low contrast. Therefore, image segmentation requires automated methods. Individual differences in the tracer uptake and a low contrast to noise ratio typical to PET images are significant challenges for the segmentation. However, time dependent information about tracer uptake present in dynamic PET studies can be used to improve the segmentation of the PET images.

There are some studies addressing automatic segmentation of dynamic PET brain images with basic pattern classification methods. For example in [2] dynamic PET images are segmented using an expectation-maximization type algorithm and Markov random field models. In [7] dynamic PET brain images are segmented with an algorithm similar to the K-means clustering algorithm. In this study, we evaluate and compare pattern recognition methods (expectation-maximization algorithm, fuzzy C-means algorithm and independent component analysis) for automatic segmentation of PET brain images.

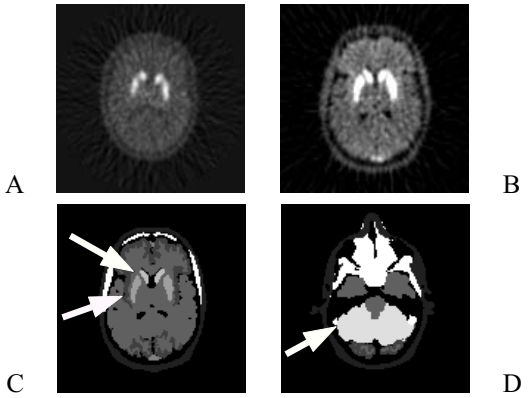

Fig. 1: Examples of transaxial image cross-sections A) from the 8th time frame of a PET study, B) from the 8th time frame of a phantom study. Examples of cross-sections of the Zubal brain phantom: C) Striatum (consists of left and right caudate nuclei and left and right putamen), D) Cerebellum.

II. MATERIALS AND METHODS

A. Dynamic PET Images

We evaluated selected algorithms using a phantom image simulated with Monte Carlo simulator and dynamic PET brain studies of five different subjects. The image sizes were $128 \times 128 \times 63$ voxels for the phantom image and $128 \times 128 \times 35$ for the human PET studies. We had these 3-D images from 13 different time intervals. The tracer in the PET imaging was C-11 Raclopride. The images were reconstructed with the FBP (Filtered Back Projection) method. With the phantom image we were able to compare algorithms quantitatively whereas the human studies allowed us to study the influence of individual differences in tracer uptake to the segmentation results. Example cross-sections of the phantom image, a human PET image and the anatomical Zubal phantom are shown in Figure 1.

The phantom image was generated by using SORTEO Monte Carlo simulator [6] based on the anatomical Zubal phantom [8]. This Monte Carlo -based simulation tool is dedicated to full ring tomographs. It is able to generate realistic 2-D and 3-D emission and transmission projections in accordance with the numerical representations of the activity and attenuation media distributions as well as the scanner geometry and physical characteristics. The simulation model accounts for most of the phenomena encountered during PET acquisitions including the Poisson nature of the emission, positron range in tissues, annihilation protons non-collinearity, scatter, randoms and system dead-time.

B. Classification Problem

The aim is to extract striatum and cerebellum from dynamic PET brain images. We assume that there are eight functionally different brain structures present in the images. Therefore, the number of clusters for classification algorithms is nine (8 structures and the background cluster). The data consists of time activity curves (TACs) $x_i(t)$ for each voxel i. However, we have no information about continuous time activity curves, only a vector of measured activities at distinct time intervals $\Delta t_1, \ldots, \Delta t_k$ $\boldsymbol{x}_i = [x_i(\Delta t_1), \ldots, x_i(\Delta t_k)]$ for each voxel i ($k = 13$). These vectors are the input for the classification algorithms.

Due to significant individual differences in the radioactivity levels, supervised classifier for PET image segmentation would have to be trained separately for each image. Therefore, only unsupervised classification is considered because we are after automatic image segmentation. The algorithms considered in this study are expectation-maximization (EM) algorithm, fuzzy C-means algorithm (FCM) and independent component analysis (ICA).

C. Classification Methods

1) Expectation-Maximization Algorithm:
The expectation-maximization (EM) algorithm is an iterative procedure for maximum-likelihood (ML) estimation of parameters of a multivariate Gaussian mixture model [1], [4]. Assuming that the TACs $\boldsymbol{x}_i$ in each class are normally distributed, this allows for specifying class conditional probability densities. After that voxels can be classified by using a Bayes classifier.

The ML estimation aims to find parameter values that maximize the probability of the observed time activity curves. This is done by the EM algorithm. During the estimation step of the algorithm, the probabilities of a voxel belonging to certain class are computed using current estimate of the probability function for the class. During the maximization step, the new probability functions for each class are computed. These steps are iterated until a local maximum of the likelihood function is found. The algorithm is guaranteed to converge to a local maximum [3].

2) Fuzzy C-Means Algorithm:
Fuzzy C-means (FCM) algorithm is an iterative procedure which approaches the classification problem by calculating membership grades for voxels [4]. This is achieved by minimizing cost function

$$J_{FCM} = \frac{1}{2} \sum_{i=1}^{9} \sum_{j=1}^{n} (U[i,j])^m \|\boldsymbol{x}_j - \boldsymbol{w}_i\|^2 \qquad (1)$$

with respect to membership grades $U[i,j] \in [0,1]$ and clustering centroids $\boldsymbol{w}_i$. The fuzzification parameter m defines the degree of "fuzziness", i.e. how much of a voxel can be classified to several classes. Voxels are classified to clusters by their maximum membership grades. The cost function in Eq. (1) implies that time activity values for each voxel $x_i(\Delta t_1), \ldots, x_i(\Delta t_k)$ are assumed to be uncorrelated and have equal variance.

3) Independent Component Analysis:
Independent component analysis (ICA) is a statistical method for transforming an observed multidimensional random vector into components that are statistically as independent from each other as possible [5]. In this case observations are time activity curves $\boldsymbol{x}_i$ and independent components (ICs) are 3-D images representing functionally different brain structures. These ICs are rarely binary valued and therefore in order to achieve segmentation of brain images the IC images have to be thresholded. In this work, the threshold value for each IC image is selected manually.

ICA assumes that distributions of ICs are non-Gaussian and statistically independent. Note that these assumptions do not directly concern classes. For solving independent component analysis we use FastICA [5] algorithm which is based on minimization of criterion derived from the concept of mutual information. Note that there is no way for determining either the order of the separated ICs or their magnitudes.

D. Evaluation

The segmentation results of phantom studies were examined quantitatively by comparing the segmentation results to anatomical ground-truth (Zubal brain phantom). The applied criteria were miss classification rate and Tanimoto coefficient values for each brain structure of interest. The miss classification rate describes how large percentage of voxels is incorrectly classified compared to the total number of voxels, i.e. the smaller the miss classification rate the better the classification result. Similarity of a particular extracted brain structure and the anatomical ground-truth can be assessed by Tanimoto coefficient. Assume n_1 and n_2 are the numbers of voxels in sets S_1 and S_2, respectively, and n_{12} is the number of voxels that are in both S_1 and S_2. The Tanimoto coefficient is then defined as

$$D_{Tanimoto}(S_1, S_2) = \frac{n_{12}}{n_1 + n_2 - n_{12}}. \qquad (2)$$

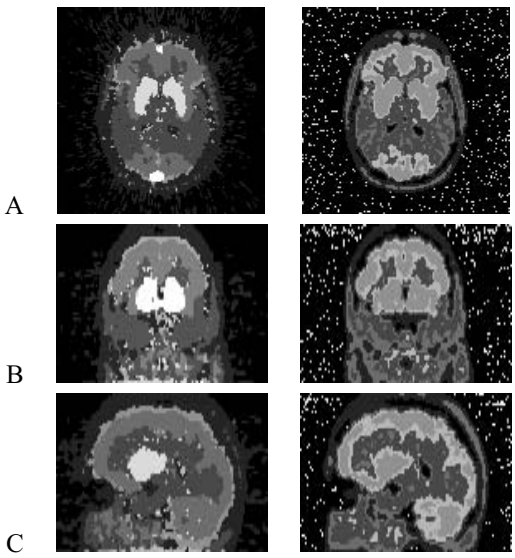

Fig. 2: Phantom results by using EM algorithm (on left) and FCM algorithm (on right). A) transaxial view, B) coronal view and C) sagittal view. The FCM algorithm classifies the striatum and the grey matter to a same class so the striatum has different grey level in the images on right than in the images on left.

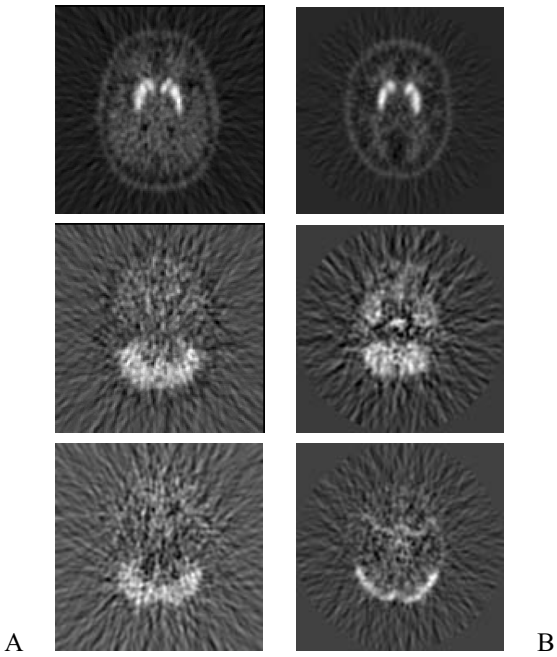

Fig. 3: Results of the FastICA. A) Phantom study, B) best result from human PET images. From top transaxial cross-sections of independent components corresponding to specific bounding (striatum), unspecific bounding (cerebellum) and blood pool.

The greater the Tanimoto coefficient the better is the result.

III. Results

The segmentation algorithms (EM, FCM and FastICA) were applied to the phantom image and to the PET studies described in Section II. The striatum was extracted with the EM algorithm and FastICA from phantom and human studies. The cerebellum was separated only with FastICA from phantom studies. The EM and FCM algorithm classified cerebellum to same class with the grey matter. The FCM algorithm classified also the striatum to that class. The results with the phantom image express how accurate segmentations of structures can in principle be achieved with human data. These results were evaluated quantitatively and the quantitative results are in Table 1. The values of Tanimoto coefficients and miss classification rates indicate that the results of the FCM algorithm were slightly better than the results of the EM algorithm. However, the striatum was not classified to its own class by FCM and therefore we were not able to compute Tanimoto coefficient for it. The Tanimoto coefficient values of FastICA were considerably better than the corresponding values of EM or FCM algorithms. However, the thresholding step required by FastICA (cf. Section IIC) was performed manually whereas other algorithms were completely automatic.

By the EM algorithm we were able to separate striatum and cerebellum from the phantom study satisfactorily. Striatum separated by the EM algorithm is presented in Figure 2A (in white). The striatum structure extracted by the EM algorithm corresponded only approximately to the anatomical structure of the Zubal brain phantom. Note especially that sagittal sinus was classified to the same class as striatum as can be seen from transaxial cross-section in Figure 1A. The EM algorithm was unable to distinguish between cerebellum and grey matter. However, grey matter and cerebellum were quite well extracted from the rest of the brain. The striatum was separated approximately by the EM algorithm from all five human PET studies. An example segmentation result is shown in Figure 5A. Cerebellum could not be extracted from any of the PET studies by the EM algorithm.

By using fuzzy C-means algorithm we were unable to separate striatum from the white matter from phantom studies as can be seen from Figure 2B. Also a part of the voxels in cerebellum (but not all) were classified to the same class as striatum. Cerebellum and grey matter could not be differentiated by the FCM algorithm. From the human PET studies the FCM algorithm was not able to separate striatum nor cerebellum to their own classes as can be seen from Figure 5B. The region of spinal fluid between the skull and the brain was separated from the PET studies (the thin dark line in between lighter shades of grey in Figure 5B).

The results of FastICA were nine images representing

Table 1: Tanimoto coefficients of found structures and miss classification rates for Phantom studies.

	EM	FCM	FastICA
Miss classification rate	0.3265	0.2644	–
Background	0.7660	0.8362	–
Grey matter	0.3991	0.4193	–
Striatum	0.3576	–	0.6533
Cerebellum	0.1347	0.1439	0.4860
Cerebellum and grey matter	0.5180	0.4858	–

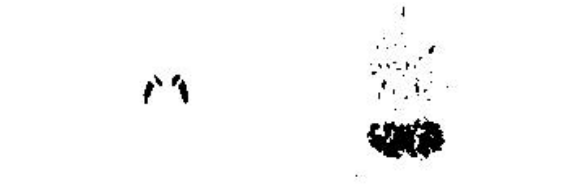

A B

Fig. 4: Thresholded independent components from the phantom study. A) Striatum, B) Cerebellum.

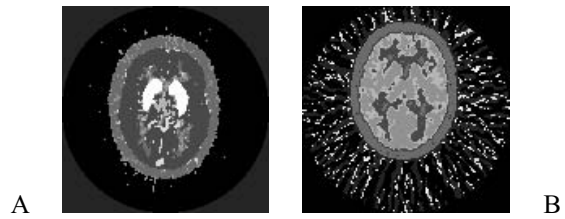

A B

Fig. 5: The best result of human PET studies by using A) the EM algorithm and B) the FCM algorithm.

independent regional components. In other words FastICA does not provide segmentations directly. With the phantom image, the independent components corresponding striatum and cerebellum structures matched well to the ground-truth anatomy (see Figure 3). Striatum and cerebellum extracted by manually thresholding the independent component images are shown in Figure 4. From the human brain studies generated IC images corresponding to the functional structure of striatum and blood pool were promising. The cerebellum could not be extracted from the human brain studies.

With the human PET images, it was observed that results of FastICA were least sensitive to noise. The EM algorithm seemed to be most sensitive to patient movement during the study and it was also most sensitive to noise.

IV. Discussion

The aim of this study was to compare pattern classification methods in automatic segmentation of dynamic PET brain images. The EM algorithm, the FCM algorithm and FastICA were selected as classification algorithms because they have turned out to be useful methods with similar problems. We would like to emphasize that the segmentation was performed by using information about dynamics of tracer uptake.

All three studied methods presented an identifiability problem. This means that the order of interesting components or classes were not always the same, i.e. striatum could be in the first class with one PET study and in the second with another PET study. The identifiability problem seems to be more easily solved in the case of clustering methods than in the case of ICA. With ICA the problem was that independent components contained voxels from several brain structures. However, as can be seen from Figure 3, the highest intensities in the specific bounding independent component relate to the striatum. Also, the thresholding of independent components has to be automated for automatic segmentation of brain images using ICA.

The EM algorithm and ICA seemed promising for the segmentation task in a sense that reasonable segmentation results were achieved when low contrast to noise ratio of the images is taken into account. The FCM algorithm could not separate structures of our primary interest (striatum and cerebellum). However, the miss classification rate by the FCM algorithm was better than with the EM algorithm with the phantom study. The merits of the different algorithms were found to be distinct and therefore it would be interesting to study the combination of the methods. To conclude, we found that most accurate results (i.e. volumes) were obtained by ICA but the level of automation of ICA was somewhat lower than with the other algorithms due to required thresholding.

Acknowledgements

The authors wish to thank Turku PET Centre for providing the PET data. The Academy of Finland and Tekes Drug2000 Technology Program are acknowledged for the financial support. We wish to thank Anthonin Reilhac (Montreal Neurological Institute, Canada) for providing the Monte Carlo simulated phantom.

References

[1] Jeff A. Bilmes, "A Gentle tutorial of the EM algorithm and its application to parameter estimation for Gaussian mixture and hidden Markov models", Technical report, International Computer Science Institute, Berkeley California, 1998 (http://ssli.ee.washington.edu/people/bilmes/mypapers/em.pdf)

[2] J. L. Chen, S. R. Gunn, M. S. Nixon and R. N. Gunn, "Markov random field models for segmentation of PET images", M. F. Insana, R. M. Leahy (Eds.): In proc. of IPMI2001, LNCS 2082, pp. 468-474, 2001

[3] A. P. Dempster, N. M. Laird and D. B. Rubin, "Maximum Likelihood from incomplete data via the EM algorithm", Journal of Royal Statistical Society, Vol. B39, pp. 1-38, 1977

[4] R. O. Duda, P. E. Hart and D. G. Stork, Pattern Classification, Second Edition, Wiley-Interscience, 2001

[5] A. Hyvärinen, J. Karhunen and E. Oja, Independent Component Analysis, Wiley-Interscience, 2001

[6] A. Reilhac, C. Lartizien, N. Costes, S. Sans, C. Comtat, R. Gunn and A. Evans, "PET-SORTEO: A Monte Carlo-based simulator with high count rate capabilities", IEEE Trans. Nucl. Sci., Vol. 51, No. 1, pp. 46-52, 2004

[7] K-P Wong, D. Feng, S. R. Meikle and M. J. Fulham, "Segmentation of dynamic PET images using cluster analysis", IEEE Transactions on nuclear science, Vol. 49, No. 1, pp. 200-207, 2002

[8] I. Zubal, C. Harrell. E. Smith, Z. Rattner, G. Gindi, and P. Hoffer, "Computerized three-dimensional segmented human anatomy", Med. Phys., Vol. 21, No. 2, pp. 299-302, 1994